HHS Public Access

Author manuscript

Invest New Drugs. Author manuscript; available in PMC 2015 August 01.

Published in final edited form as:

Invest New Drugs. 2014 August ; 32(4): 604–617. doi:10.1007/s10637-014-0084-7.

Oxidative cytotoxic agent withaferin A resensitizes temozolomide-resistant glioblastomas via MGMT depletion and induces apoptosis through Akt/mTOR pathway inhibitory modulation

Patrick T. Grogan[a,b], **Jann N. Sarkaria**[c], **Barbara N. Timmermann**[d], and **Mark S. Cohen**[a,b,*]

[a]Department of Pharmacology, Toxicology, and Therapeutics, University of Kansas Medical Center, Kansas City, Kansas 66160, USA

[b]Department of Surgery, University of Michigan Hospital and Health Systems, Ann Arbor, Michigan 48109, USA

[c]Department of Radiation Oncology, Mayo Clinic, Rochester, Minnesota 55905, USA

[d]Department of Medicinal Chemistry, University of Kansas School of Pharmacy, Lawrence, Kansas 66045, USA

Abstract

Temozolomide (TMZ) has remained the chemotherapy of choice in patients with glioblastoma multiforme (GBM) primarily due to the lack of more effective drugs. Tumors, however, quickly develop resistance to this line of treatment creating a critical need for alternative approaches and strategies to resensitize the cells. Withaferin A (WA), a steroidal lactone derived from several genera of the *Solanaceae* plant family has previously demonstrated potent anti-cancer activity in multiple tumor models. Here, we examine the effects of WA against TMZ-resistant GBM cells as a monotherapy and in combination with TMZ. WA prevented GBM cell proliferation by dose-dependent G2/M cell cycle arrest and cell death through both intrinsic and extrinsic apoptotic pathways. This effect correlated with depletion of principle proteins of the Akt/mTOR and MAPK survival and proliferation pathways with diminished phosphorylation of Akt, mTOR, and p70 S6K but compensatory activation of ERK1/2. Depletion of tyrosine kinase cell surface receptors c-Met, EGFR, and Her2 was also observed. WA demonstrated induction of N-acetyl-L-cysteine-repressible oxidative stress as measured directly and through a subsequent heat shock response with HSP32 and HSP70 upregulation and decreased HSF1. Finally, pretreatment of TMZ-resistant GBM cells with WA was associated with O6-methylguanine-DNA methyltransferase (MGMT) depletion which potentiated TMZ-mediated MGMT degradation. Combination treatment with both WA and TMZ resulted in resensitization of MGMT-mediated TMZ-resistance but not resistance through mismatch repair mutations. These studies suggest great clinical potential for the

[*]**Corresponding Author:** Associate Professor of Surgery Director of Endocrine Surgery Research Section of General Surgery 2920K Taubman Center, SPC 5331 University of Michigan Hospital and Health Systems 1500 E. Medical Center Drive Ann Arbor, MI 48109-5331 Telephone: +1 7346154741 Fax: +1 7349365830 cohenmar@med.umich.edu.

Conflict of Interest Disclosure: None related to this work.

utilization of WA in TMZ-resistant GBM as both a monotherapy and a resensitizer in combination with the standard chemotherapeutic agent TMZ.

Keywords

Withaferin A; glioblastoma multiforme; temozolomide resistance; oxidative stress; heat shock response; Akt/mTOR pathway; O6-methylguanine-DNA methyltransferase

Introduction

According to the American Cancer Society, over 23,000 new cases of brain and other nervous system tumors will be diagnosed in 2013 in the United States [1]. High grade gliomas, such as anaplastic astrocytoma and glioblastoma multiforme (GBM), account for approximately 38% of primary brain tumors, and to date, treatment options have remained limited. Following optimal surgical debulking, radiation therapy alone has been shown to increase mean survival time of GBM patients from approximately six months to only one year [2-4]. Concomitant and adjuvant temozolomide (TMZ) with surgical debulking and radiotherapy represents the most effective approved treatment in GBM patients but still only yields a 2.5 month median survival benefit and two year survival rate of 26.5% [5-9].

The efficacy of TMZ is most frequently influenced by the methylation status of the *MGMT* (O6-methylguanine-DNA methyltransferase) gene promoter [10, 11]. In patient tumors with an unmethylated promoter, the MGMT protein is expressed and repairs the major O6-methylguanine cytotoxic DNA lesions caused by TMZ, essentially eliminating its anti-cancer efficacy [12, 13]. Fifty-five to sixty-five percent of glioma patients do not display tumor phenotypes favorable for treatment with TMZ, and those that do often quickly acquire resistance through acquisition of MGMT or mismatch repair (MMR) deficiencies that allow tolerance of the lesion [14-16].

To date, experimental targeted therapies against proteins such as epidermal growth factor receptor (EGFR), mammalian target of rapamycin (mTOR), and PI3 kinase have yielded disappointing responses in GBM patients despite promising pre-clinical findings [14, 17]. Combined with the limitations of TMZ, this defines a critical need for improved diagnostic and therapeutic approaches for patients with both inherent and acquired TMZ resistance to either promote resensitization of the malignancy to TMZ or exploit unrelated vulnerabilities.

The 28-carbon steroidal lactone withaferin A (WA; Fig. 1a), extracted from several genera of the *Solanaceae* plant family, has emerged as a promising anti-cancer chemotherapeutic agent with thiol-reactive and oxidative properties that exploit redox alterations in cancer cells [18-23]. As such, it has demonstrated the ability to modulate many pathways involved in promoting cancer progression including specific proteins like heat shock protein (HSP) 90, Akt, NFkappaB, and the estrogen receptor (ER) [24-34]. Promising anti-tumor efficacy has been observed in prostate, thyroid, breast, melanoma, ovarian, cervical, and brain cancer models [19, 32, 35-40].

Here, we follow-up on our previous findings outlining the efficacy of WA in TMZ-sensitive glioblastoma cells lines to demonstrate its potential role as a novel therapeutic option against resistant tumors as both a single agent therapy and a TMZ-resensitizer through MGMT modulation.

Materials and Methods

Cell culture and general reagents

U87, U251, and T98G glioblastoma multiforme cell lines of human origin were grown in Dulbecco's modified Eagle's medium (DMEM #11995-065; Gibco, Grand Island, NY) supplemented with 10% fetal bovine serum (FBS; Sigma-Aldrich, St. Louis, MO) and 1% penicillin/streptomycin (Sigma-Aldrich, St. Louis, MO) in a 37°C humidified atmosphere of 5% CO_2 in air. An additional human GBM cell line, U138, was maintained in equivalent media additionally supplemented with 2% L-glutamine (200 mM; Sigma-Aldrich), 1% MEM-vitamin (100x; Hyclone, Logan, UT), and 1% MEM nonessential amino acids (Sigma Aldrich). The TMZ resistant cells U87TMZ and U251TMZ were derived as previously described via TMZ dose escalation from the parental U87 and U251 cells, respectively [41].

TMZ was generously provided by the NCI Developmental Therapeutics Program (Bethesda, MD) and was stored as a 100mM stock solution in DMSO at −80°C. Withaferin A (99% pure by HPLC) was extracted, isolated, and stored as a 20mM stock solution in DMSO at −80°C as previously described [42]. Propidium iodide (PI), RNase, N-acetyl-L-cysteine (NAC), protease inhibitor cocktail, and MEK inhibitor PD98059 were acquired from Sigma-Aldrich (St. Louis, MO). Annexin V-FITC was obtained from BD Biosciences (San Diego, CA). Caspase 8 inhibitor Z-IETD-FMK and caspase 9 inhibitor Z-LEHD-FMK were obtained from R&D Systems (Minneapolis, MN).

MTS assay

To determine the IC_{50} values of WA, all cell lines were seeded in 96-well plates at a density of 2,500 cells/well, treated with 0.025-3μM WA, and incubated for 72h. Cell number and viability were quantified by the colorometric CellTiter96 Aqueous MTS assay (Promega, Fitchburg, WI) at 490nm on a BioTek Synergy 2 plate reader (BioTek, Winooski, VT) as per the manufacturer's instructions.

To assess combinational effects of WA and TMZ, cells were plated in 75cm^2 flasks and allowed to grow overnight. Cells were treated with 0.5-2μM WA and harvested at 24, 48, and 72h post-treatment (60-80% confluency) for seeding in 96-well plates at densities of 500-10,000 cells/well. Following a 6h incubation period, 10-50μM and 100-500μM TMZ were added to each well of the TMZ-sensitive and TMZ-resistant cells, respectively. After 48-144h, cell number and viability were quantified by the MTS assay as described above.

CellTiter-Glo luminescent assay

To circumvent the auto-reductive potential of NAC that interferes with the MTS assay reagent, studies evaluating combination treatment with NAC and WA were completed with the CellTiter-Glo luminescent assay (Promega, Fitchburg, WI) measuring cell viability by

adenosine triphosphate (ATP) levels. U251TMZ and U87TMZ cells were seeded at a density of 2,500 cells/well in white-chambered 96-well plates and allowed to incubate for 6h before treatment with 1-5mM NAC. After 1h, 0.5-6μM WA was added to each well. After 72h, assay reagent was prepared and added as per the manufacturer's instructions, and the plates were evaluated on the BioTek Synergy 2 plate reader.

Cell cycle analysis

U251TMZ and U87TMZ cells were plated and allowed to grow overnight to 30-50% confluency. Cells were treated with 0.125-4μM WA for 24h. Cells were then collected, resuspended in 0.43mL of 4°C 1x PBS followed by 1mL of −20°C ethanol, and maintained at −20°C for a minimum of 24h. Finally, cells were then pelleted by centrifugation, resuspended in 1x PBS with 40ug/mL PI and 100ug/mL RNase, and incubated at 37°C for 30 minutes before analysis by flow cytometry (BD LSRII; Becton Dickinson, San Diego, CA). Data analysis included only singlet living cells not displaying DNA fragmentation.

Apoptosis studies

Cells were plated as described for cell cycle analysis, treated with 1-6μM WA, and pre-treated for 1h with 5mM NAC where indicated. After 24h, cells were collected and washed once with Annexin binding buffer as previously described [34]. Staining phosphatidylserine on the outer leaflet of the cell membranes on apoptotic cells with Annexin V-FITC and DNA staining by PI in necrotic and late apoptotic cells was performed to assess WA-induced cell death. Cells were stained with both compounds according to the manufacturer's instructions (BD Biosciences, San Diego, CA) for 15 minutes at 4°C and washed twice with Annexin binding buffer. Cells were resuspended in buffer and immediately analyzed by flow cytometry on the BD LSRII.

Immunoblotting

Cells were plated in the manner outlined for cell cycle analysis and treated with 0.5-5μM WA. Where indicated, cells were either pre-treated with 5mM NAC, 50μM PD98059, 50μM Z-IETD-FMK, or 50μM Z-LEHD-FMK for 1h or post-treated with 100-300μM TMZ 24h after WA. After 24-48h, proteins were collected in lysis buffer (40mM HEPES, 2mM EDTA, 10mM sodium pyrophosphate decahydrate, 10mM β-glycerophosphate disodium salt pentahydrate, 1% Triton X-100 supplemented with 100μM phenylmethylsulfonyl fluoride, 1mM Na_3VO_4, and 2μL/mL protease inhibitor cocktail), quantified, separated by sodium dodecyl sulfate–polyacrylamide gel electrophoresis (SDS–PAGE), and electrotransfered onto a Hybond nitrocellulose membrane as previously described in Samadi, et al. [43]. 10-80μg of protein sample was utilized per lane. Actin levels were used to ensure equal loading and transfer of proteins. All studies were repeated for accuracy.

Primary rabbit antibodies against MGMT (#2739; 1:5000), MSH2 (#2017; 1:1000), and MSH6 (#3996; 1:1000) and primary mouse antibody against MLH1 (#3515; 1:1000) were acquired from Cell Signaling Technology (Beverly, MA). Primary mouse antibody against p-H2A.X (Ser139; #613401; 1:1000) was purchased from Biolegend (San Diego, CA). Additional primary and secondary antibodies were utilized as previously described at dilutions ranging from 1:250-1:5000 and 1:5000-1:20000, respectively [34].

Evaluation of reactive oxygen species

The accumulation of intracellular peroxide-type reactive oxygen species (ROS) in U251TMZ and U87TMZ cells was determined using the general oxidative stress indicator CM-H_2DCFDA (Molecular Probes, Grand Island, NY) that fluoresces upon oxidation. Cells were incubated at 37°C in 1x dPBS containing 20μM CM-H_2DCFDA for 1h to allow for indicator preloading and plated in 96-well plates in phenol red-free DMEM at 20,000 cells/well. After 30 minutes, 1-5μM WA and/or 5mM NAC was added to the wells. Fluorescence was assessed on the BioTek Synergy 2 3h post-treatment with excitation and emission filters of 485nm and 528nm, respectively.

Statistical analysis

GraphPad Prism 6 (version 6.02; GraphPad Inc., San Diego, CA) was used to generate best-fit non-linear sigmoidal dose response curves for IC_{50} determination. Comparisons of differences between two or more means/values were determined by Student's unpaired t-test via the statistical functions of GraphPad Prism and Microsoft Excel 2010 software (version 14.0.6129.5000; Microsoft Corporation Redmond, WA). Densitometry, where indicated, was completed using ImageJ software (version 1.46r; Bethesda, MD). Combination studies compared drug efficacy within normalized WA treatment arms. Data are presented as mean values with error bars denoting standard deviation or standard error of the mean where appropriate. Unless otherwise noted, all experiments were performed minimally in triplicate. The level of significance was set at $p<0.05$.

Results

Characterization of TMZ resistant cell lines

U251 and U87 resistant sub-lines (U251TMZ and U87TMZ) were generated by exposing parental lines to increasing concentrations (30-300μM) of TMZ over an 8-week period, pooling the resulting colonies, and confirming resistance as previously described [41]. Reduced TMZ effectiveness in established lines T98G and U138 has been previously confirmed [44]. Characterization of these cell lines demonstrated the absence of MGMT and the presence of mismatch repair proteins MLH1, MSH2, and MSH6 in parental U251 and U87 cells (Fig. 1b). MGMT expression was observed in U251TMZ, T98G, and U138 cells but not U87TMZ. Compared to parental U87 cells, U87TMZ displayed lower levels of all three MMR proteins screened, suggesting the mechanism of U87TMZ resistance is due to heterogeneic deletion or mutation of these proteins.

Diminished cell proliferation and viability following withaferin A exposure

To evaluate the general cytotoxic effect of withaferin A, parental and resistant glioblastoma cells were treated with increasing concentrations of WA (0.025-3μM) for 72h with resulting cell number and viability determined by MTS assay (Fig. 1c). WA dose escalation reduced cell proliferation and viability. By GraphPad analysis, the IC_{50} values of TMZ resistant sub-lines U251TMZ and U87TMZ were lower compared to parental lines, demonstrating increased efficacy. IC_{50} values were determined to be 0.766±0.045μM, 0.357±0.019μM,

1.050±0.062μM, 0.657±0.134μM, 1.027±0.105μM, and 0.610±0.279μM for U251, U251TMZ, U87, U87TMZ, T98G, and U138 cells, respectively.

Induction of G2/M cell cycle arrest by withaferin A in a dose-dependent manner

Distribution of phases of the cell cycle was assessed by flow cytometry at 24h. Consistent with the anti-proliferative effects seen in the MTS assays, WA treatment induced G2/M phase accumulation of U251TMZ and U87TMZ cells in a dose-dependent manner, demonstrating a key cellular response to WA exposure. WA induced a dose-dependent shift in cell cycle arrest from the G0/G1 checkpoint to G2/M arrest with minimal change in the percentage of cells in S phase (Fig. 2a). Maximal shift to G2/M arrest above baseline was observed at 1.5μM in U87TMZ cells (17.8% G2/M in controls increasing to 42.5% with treatment; p=0.0001) and 2μM in U251TMZ cells (43.1% baseline to 72.3% with treatment; p=0.0001) (Fig. 2b). Doses above this level demonstrated diminished deviation from control with a return to higher G0/G1 and lower G2/M but also increased DNA fragmentation observed in the sub-G0/G1 region (data not presented).

Additionally, cyclin B_1, a protein that displays G2/M phase-specific elevation, was evaluated by Western blotting to provide molecular confirmation of increases in G2/M cell cycle arrest. At 24h, dose-dependent induction of cyclin B_1 was observed in both U87TMZ and U251TMZ cells with maximum expression levels observed at 1μM and 2.5μM WA, respectively, corresponding with flow cytometry findings (Fig. 2c). Cyclin B_1 levels displayed similar peak expression levels at 48h but with a more blunted response.

Withaferin A induces cell death through both the intrinsic and extrinsic apoptotic pathways

PI and Annexin V-FITC dual staining analysis with flow cytometry was used to further characterize the anti-proliferative effects of WA by assessing levels of apoptosis and necrosis following drug exposure. After 24h of 1-3μM WA, U87TMZ and U251TMZ cells demonstrated increases in Annexin V-only staining representative of early apoptotic processes with increases in dual staining representative of late apoptosis present at higher concentrations (2-6μM) (Figs. 3a and 3b). U87TMZ cells alone appear to also show mild increases in levels of necrosis with WA exposure as demonstrated by staining with PI only. Total positive staining of control U87TMZ and U251TMZ cells was 8.2% and 4.0% but increased to 45.5% (p=0.01: 14.7% early apoptosis; 23.0% late apoptosis; 7.7% necrosis) and 17.1% (p=0.0004: 9.1% early apoptosis; 6.9% late apoptosis; 1.0% necrosis) with 2μM WA, respectively. 6μM WA elevated total cell death to 80.0% for U87TMZ (p<0.0001: 4.9% early apoptosis; 62.6% late apoptosis; 12.5% necrosis) and 51.8% for U251TMZ cells (p<0.0001: 4.0% early apoptosis; 44.6% late apoptosis; 3.1% necrosis).

Molecular confirmation of an apoptotic response was conducted by Western blotting for cleaved and/or total levels of the following proteins: extrinsic procaspase 8, mitochondrial/intrinsic procaspase 9, effector procaspases 3 and 7, and downstream poly(ADP-ribose) polymerase (PARP) cleavage (Fig. 3c). At 24h, increasing concentrations of WA resulted in progressively decreased levels of all procaspases and PARP, suggesting both intrinsic and extrinsic routes of apoptotic cell death. Maximum levels of cleaved caspase 8 were observed

at 1-2.5μM WA for U251TMZ and 0.5-1μM WA for U87TMZ while highest levels for cleaved caspases 3 and 7 were observed at 5μM WA for U251TMZ and 1-2.5μM WA for U87TMZ. PARP cleavage increased up to 5μM in both cell lines, the maximum concentration utilized, and suggests that the absence of cleaved caspases despite depletion of the procaspase form at high WA concentrations can be explained by a time-dependent nature of caspase signaling in which the upstream cleaved caspases are ultimately degraded following their activity.

To further evaluate the nature of the intrinsic and extrinsic apoptotic processing in WA-induced cytotoxicity, U251TMZ cells were pretreated with 50μM of either caspase 8 inhibitor Z-IETD-FMK or caspase 9 inhibitor Z-LEHD-FMK for 1h followed by 2.5μM WA for 24h. Pretreatment with both inhibitors resulted in a return to baseline for both cleaved caspase 3 and PARP levels and decreased amounts of cleaved caspase 7 compared to WA alone (Fig. 3d). Inhibitors alone resulted in negligible changes. These data support that cytotoxicity at WA concentrations above IC_{50} involves induction of intrinsically- and extrinsically-mediated apoptosis in the GBM cell lines tested.

Withaferin A modulates the Akt/mTOR and MAPK pathways

Proteins in and related to the Akt/mTOR and mitogen-activated protein kinase (MAPK) pathways are key to proliferation and survival of GBM cells and other cancers [17]. These proteins were evaluated by Western blotting at 24-48h post-treatment in U251TMZ and U87TMZ cells in order to evaluate WA activity against total and phosphorylated protein levels as a potential mechanism for the anti-proliferative effects observed (Fig. 4a). At 24h, total levels of Akt and mTOR were decreased between ~1-5μM WA with minimal changes occurring in total p70 S6 kinase (S6K) in both cells lines. However, activation of each protein via phosphorylation (p-Akt Ser473, p-mTOR Ser2448, and p-p70 S6K Thr389) was similarly reduced over this range. Phosphorylation at Thr412 of the nuclear isoform of p70 S6K, p85 S6K, was also reduced with increasing WA concentration (data not shown). These effects were observed through the 48h timepoint and demonstrate an inhibitory effect of WA on the Akt/mTOR growth pathway. Additionally, phosphorylation (Thr172) of AMPKα, the catalytic subunit of a negative regulator of the Akt/mTOR pathway that responds to cellular stressors, was increased with WA treatment, peaking at 1μM in U251TMZ cells (Online Resource 1). Despite depletion of total levels of the downstream tumor suppressor TSC2, phosphorylation at Thr1462 was enhanced or maintained at all WA concentrations tested in U251TMZ cells. In contrast to previous observations in parental U87 cells [34], total and phospho- levels of AMPKα were decreased in U87TMZ cells despite maintenance of p-TSC2 levels (Online Resource 1).

The MAPKKK Raf-1 and the MAPK ERK2 were assessed to evaluate the effects of WA on the primary proliferative MAPK pathway (Fig. 4a). Total Raf-1 levels decreased at ~2.5-5μM in both U251TMZ and U87TMZ cells, however, activating phosphorylation of the protein at Ser338 increased over the same concentration range. Downstream, minimal changes were observed in total ERK2 levels, but phosphorylation of ERK1/2 (Thr202/Tyr204) was notably increased in a dose-dependent manner in both cell lines with a maximum level achieved at 2.5μM WA in each at both 24h and 48h. Given that

phosphorylation of MAPK proteins is typical of a pro-survival response yet WA instead induces apoptosis in GBM cells, the MAPK pathway was further explored to determine if its activation was necessary for the induction of apoptosis or simply a compensatory pro-survival response. U251TMZ and U87TMZ cells were pretreated with 50μM of the MAPKK MEK inhibitor PD98059 for 1h followed by 2.5μM WA for 6h or 24h. Pretreatment with the inhibitor alone resulted in increased ERK1/2 phosphorylation but limited WA-induced phosphorylation in a time-dependent manner (Fig. 4b). Alterations in apoptosis were assessed by cleaved caspase 3 and cleaved PARP levels. WA alone induced observable caspase 3 and PARP cleavage at 24h in both cell lines and PARP cleavage alone at 6h in U87TMZ. However, cleaved caspase 3 and PARP levels were increased when combined with the MEK inhibitor at 24h in U251TMZ and 6h in U87TMZ, demonstrating that MAPK pathway activation with WA treatment appears to represent a compensatory response to the apoptotic effects induced by the compound.

Finally, the tyrosine kinase receptors EGFR, Her2/ErbB2, and c-Met, known to signal to both the Akt/mTOR and MAPK pathways, were evaluated due to their status as common amplified, mutated, and/or drug-targeted surface proteins in GBM [45-49]. Total levels of EGFR and Her2/ErbB2 in both U251TMZ and U87TMZ decreased with 2.5-5μM WA treatment at 24h and 48h while total levels of c-Met decreased at 5μM (Fig. 4a). Interestingly, increased phosphorylation of Tyr1068 on EGFR was observed at 2.5-5μM depending on the cell line as well as increased phosphorylation of Tyr1234/1235 on c-Met in U87TMZ cells up to 2.5μM WA at 48h. Phosphorylation of c-Met was otherwise downregulated with WA treatment in both lines.

Withaferin A elevates oxidative status and induces a heat shock stress response in TMZ-resistant cells

We have previously demonstrated the ability of WA to elevate oxidative potential and ROS-mediated cell death in TMZ-sensitive GBMs [34]. TMZ has also been demonstrated to produce ROS that result in inhibitory activation of AMPK [50]. We therefore evaluated the nature and ability of WA to continue to induce ROS in TMZ-resistant U87TMZ and U251TMZ cells. Peroxide-type radical production was monitored with CM-H_2DCFDA conversion at 3h post-WA exposure. Both cell lines showed statistically significant increased detectible CM-H_2DCFDA fluorescence with increasing WA exposure. ROS levels rose 20.9% ($p=0.001$), 36.6% ($p=0.002$), and 38.8% ($p=0.01$) in U251TMZ and 21.3% ($p=0.003$), 40.6% ($p=0.004$), 47.3% ($p=0.001$) in U87TMZ cells at 1, 3, and 5μM WA compared to control, respectively (Fig. 5a). The thiol antioxidant and ROS scavenger NAC was added simultaneously with WA and was shown to nearly complete abrogate WA-generated ROS, further demonstrating the nature of the effect.

Various models of oxidative stress are known to be associated with a heat shock response via induction of several HSPs [51, 52], and alteration of HSPs were previously reported following WA treatment [34, 53]. Treatment with WA yielded a unique pattern of HSP expression modulation in U251TMZ and U87TMZ cells (Fig. 5B). Total levels of HSP32/heme oxygenase 1 and HSP70, but not HSP90, were observed to increase with increasing concentrations of WA at 24h. HSP27 was depleted at 24h with 5μM WA in both cell lines

but remained largely unchanged in U251TMZ and mildly elevated in U87TMZ with other concentrations at 24h. The transcription factor heat shock factor 1 (HSF1) showed dose-dependent reduction in expression between 1-5μM WA. Pretreatment with 5mM NAC virtually eliminated all modulation of proteins in the heat shock system (Fig. 5b).

Functionally, WA-induced depletion of ATP levels, a marker of reduced cellular viability in the CellTiter-Glo assay, could be reduced or completely eliminated with 1-5mM NAC pretreatment ($p<0.0001$) (Fig. 5c). Such effects were seen with up to 6μM WA, the highest concentration examined. Additionally, re-evaluation of cell death by flow cytometry as previously described following pretreatment with 5mM NAC showed the elimination of death-associated PI and Annexin V staining normally induced by 5μM WA ($p<0.01$) (Fig. 5d). This was supported by blockage of PARP cleavage via NAC pretreatment (Fig. 5b). Additionally, WA-mediated cyclin B_1 induction was blocked by NAC, demonstrating the prevention of G2/M cell cycle arrest seen with WA treatment.

Withaferin A resensitizes TMZ-resistant GBM cells to TMZ through MGMT depletion

Expression of MGMT is associated with TMZ resistance in GBMs and therefore is an attractive target for TMZ resistance resensitization and prevention [13]. WA demonstrated the ability to induce depletion of MGMT at 48h in cell lines (U251TMZ, T98G, and U138) utilizing MGMT as the primary means of TMZ resistance (Fig. 6a). U251TMZ and U138 cells showed progressive depletion of MGMT from 0.5-10μM WA with approximately 5-fold and 20-fold less compared to control by 5μM, respectively. At 5μM WA treatment, there was a 43% reduction in MGMT in T98G cells with complete elimination by 10μM. U87TMZ cells, however, failed to express MGMT altogether.

To determine if these findings extended to functional resensitization of resistant cells to WA, two cells lines resistant through MGMT (U251TMZ and T98G) and one cell line displaying MGMT-independent resistance (U87TMZ) were treated with WA for 24h followed by TMZ and evaluated with the MTS assay (Fig. 6b). Both U251TMZ and T98G showed statistically significant decreases in cell viability when 1, 1.5, or 2μM WA was combined with 300 or 500μM TMZ. Pretreatment with 2μM WA followed by 300μM TMZ yielded a 32% ($p<0.0001$) and 34% ($p=0.004$) relative decrease in U251TMZ and T98G cell viability compared to TMZ or WA alone, respectively. In contrast, U87TMZ cells only demonstrated a statistically significant enhancement of combination therapy over TMZ alone – only 6% additional reduction in relative viability – with a 2μM WA and 300μM TMZ combination ($p=0.02$). 48h pretreatment with WA also demonstrated enhanced effect with significant elimination of the benefit by 72h pretreatment (data not shown). WA pretreatment did not prevent TMZ efficacy in TMZ sensitive U251 and U87 parental cells (Online Resource 2a).

Because TMZ also depletes MGMT [54], the effect of WA and TMZ combination on MGMT levels was evaluated. Combination therapy demonstrated dose-dependent synergy or potentiation to reduce total levels of MGMT in U251TMZ, T98G, and U138 MGMT-expressing cells (Fig. 6c). At 1μM WA in U251TMZ and U138 cells and 2.5μM WA in T98G cells, minimal decreases and/or increases of MGMT levels were observed. The

addition of 300μM TMZ for 24h resulted in 43%, 52%, and 34% reduction in MGMT protein levels compared to TMZ alone in U251TMZ, T98G, and U138 cells, respectively.

Phosphorylation of H2A.X as a marker of double strand DNA damage and cleavage of PARP during apoptosis were evaluated to look for molecular evidence of combinational efficacy. Both markers were elevated in the setting of increasing concentrations of WA in U251TMZ, T98G, U138, and U87TMZ cells. However, PARP cleavage was then diminished at the high levels of U87TMZ and U138 cells suggesting non-apoptotic cell death or very late apoptosis at this timepoint. Addition of TMZ was observed to increase p-H2A.X and PARP cleavage in only T98G, particularly at 1μM WA. Interestingly, despite similar or increased levels of cleaved PARP within WA treatment groups, levels of uncleaved PARP increased with TMZ treatment in each of the TMZ groups but not control in U251TMZ and T98G cells. Given the reported oxidative effect induced by TMZ [50], markers of oxidative stress including HSP32, HSP70, and p-AMPKα as well as the AMPK-influenced downstream phosphorylation of mTOR were evaluated to determine if combination of WA and TMZ demonstrated enhanced oxidative effect in GBM. While WA increased HSP32 and HSP70 levels in all lines and TMZ enhanced phosphorylation of AMPKα in U138, combination therapy did not result in additional effect and failed to further diminish mTOR activation (Online Resource 2b).

Discussion

While withaferin A has demonstrated effectiveness as a promising new therapeutic agent in a variety of cancer types including TMZ-sensitive GBM, this work is the first to explore its efficacy in a known model of drug-resistance. Here, we show for the first time that WA induces a potent cytotoxic effect against temozolomide resistant GBMs resulting in G2/M arrest and apoptosis from both the intrinsic and extrinsic systems. These findings correspond with the elevation of cellular oxidative potential and inhibitory modulation of the Akt/mTOR pathway but not the MAPK pathway.

Since its approval by the FDA, TMZ remains the standard-of-care chemotherapeutic agent in the treatment of primary GBM. Exposure to this agent results in DNA adducts such as O6-methylation of guanine which, if not removed by MGMT, can mispair with thymine. Cells with intact MMR undergo futile cycles of attempted repair with resultant replication-associated DNA double strand breaks, G2/M arrest, and ultimately apoptosis [55]. Targeting mechanisms of DNA damage repair with various inhibitors, such as those of PARP and ataxia telangiectasia mutated (ATM), has provided potentially beneficial strategies in enhancing TMZ effect, but comparatively limited effort has gone into addressing both inherent and acquired resistance to TMZ by MGMT expression or, less frequently, MMR mutation in GBM. Despite about half of patients displaying tumor phenotypes not conducive to TMZ use, it remains a first-line agent, demonstrating the need for better tumor screening techniques. Furthermore, initially responsive tumors are often quick to develop resistance to this line of therapy [14, 15].

Several experimental agents used to resensitize resistant cancer cells to TMZ or other alkylating agents – such as valproic acid [44, 56, 57], O6-benzylguanine [58, 59], IL-24

[60], and silencing oligonucleotides [61-63] – possess little practical intrinsic anti-cancer cytotoxic properties or clinical applicability, however, some do have the potential for adverse effects in the patient. Alternatively, dose-dense TMZ scheduling, used to deplete MGMT levels quickly to enhance TMZ effects, has yielded disappointing outcomes in several clinical trials [64]. In this study, WA acted as both an inherently cytotoxic agent and an enhancer of the efficacy of TMZ in MGMT-driven resistant cell lines while maintaining TMZ sensitivity in parental lines. Such data conceptually support the utility of combination therapy WA with TMZ in the first-line treatment of GBM. Such an approach should maximize anti-cancer activity across broad tumor heterogeneity. Importantly, while tumors with resistance due to MMR mutation may not be resensitized to TMZ by WA, the presence of a second cytotoxic chemotherapeutic agent may provide significant benefit in the context of ineffective TMZ treatment. It remains to be fully explored whether increased levels of p-H2A.X observed with WA treatment are a result of direct DNA damage, perhaps through an oxidative mechanism, or rather a known byproduct observed during cellular apoptosis for DNA fragmentation [65], however, preliminary results in breast cancer support a caspase-mediated mechanism (data not published). Elevated total PARP with increasing TMZ in the presence of WA in MGMT-expressing lines may indicate the necessity for increased base excision repair (BER) during combination therapy, alluding to induction of DNA damage as a reason for combinational efficacy which will need to be validated by further scientific investigation.

Several studies have implicated the role of WA in the disruption of HSP90 chaperone functions through binding to the C-terminus of HSP90 [26, 66]. While direct evidence of such an inhibitory effect has not yet been established, downstream depletion of various HSP90-related client proteins suggests that WA may indeed act at least in part as a novel HSP90 inhibitor. This could explain and support the wide-ranging effects observed in this study, including the depletion in total levels of known HSP90 client proteins such as Akt, mTOR, Raf-1, and EGFR. By depleting these key regulatory client proteins of HSP90, the normal signaling axes of multiple proliferative pathways are simultaneously modulated. MGMT, which is depleted in the presence of WA, has not, however, been reported as a client protein of HSP90. Indeed, current studies demonstrate that total levels of MGMT are not impacted by the widely-utilized HSP90-inhibitor 17-AAG until high concentrations (1-2μM) are achieved, suggesting that its stability and function are not directly maintained by HSP90 (data not shown). Santagata, et al. demonstrated the thiol reactivity of WA [19], and our results implicate an oxidative mechanism, representing an alternative means by which MGMT and other non-HSP90 client proteins may be targeted for degradation by WA. Interestingly, valproic acid, which diminishes MGMT levels, has also been shown to cause oxidative stress in glioma cell lines [67].

Induction of oxidation has become a promising mechanism by which to target cancer. Alterations in the redox potential of cancer cells due to various molecular turnover and quick replication results in increased cellular stress that can be exploited to shift cells into a state of cytotoxicity [68, 69]. This approach circumvents traditional therapeutic options such as antigen-targeting and DNA-damaging agents that have received the most attention but are often rendered useless due to rapid development of resistance. In GBM, such traditional agents have been explored in patients but have yielded unimpressive results in clinical trials

largely due to the development of tumor mutations that limit the effectiveness and/or relevance of a particular targeted therapeutic [14, 17].

In the present study, thiol-reactivity and oxidation by WA resulted in depletion of proteins in the Akt/mTOR and MAPK pathways including many cell surface receptors either through direct interaction or as a downstream effect of the inhibition of other proteins. As noted previously, other reports have shown additional pathways effected. Such an ability to target multiple pathways simultaneously with a single compound has great potential to generate an enhanced anti-cancer effect while reducing the development of resistance to a particular target. The ability to modulate multiple components of the Akt/mTOR pathway simultaneously provides a novel and important mechanism by which WA can manifest its beneficial effects against GBMs. Because of mutations in proteins like the tumor suppressor phosphatase and tensin homolog (PTEN), this pathway is frequently overactivated in GBM to drive proliferation, as shown in both U251 and U87 cells [70-72]. Interestingly, while we previously showed activation of AMPKα and downstream tumor suppressor TSC2 which act to inhibit mTOR in both U251 and U87 parental cells [34], U87TMZ appears to have lost the ability to act through this pathway which suggests direct inhibition of the Akt/mTOR axis.

WA treatment yields subsequent induction of the MAPK pathway as demonstrated by activating phosphorylation of EGFR, Raf-1, and ERK1/2. Previous studies have shown that reactive oxygen species generated by epoxide-containing compounds in GBM cells are responsible for the phosphorylation of ERK1/2 which then drives apoptosis [73]. In contrast, inhibition of this pathway prior to WA exposure yields enhanced apoptosis, suggesting that the activation of the MAPK pathway is a compensatory pro-survival response to apoptotic shifts in the cell and may be a therapeutic target that would synergistically enhance the efficacy of WA in future combinational therapy studies.

The studies presented here provide an important framework for the utilization of WA in TMZ-resistant GBM as both a monotherapy and as a resensitizer in combination with the standard chemotherapeutic agent TMZ. WA demonstrates an oxidative mechanism that leads to anti-proliferative and pro-apoptotic effects largely through Akt/mTOR pathway modulation. Simultaneously, depletion of MGMT allows for enhanced activity of TMZ. While future pre-clinical animal studies will be necessary to determine its translational potential in GBMs, evidence is supportive of a future clinical potential for the utilization of WA across the heterogeneic spectrum of glioma patients.

Supplementary Material

Refer to Web version on PubMed Central for supplementary material.

Acknowledgments

We would like to recognize Huaping Zhang (University of Kansas) for his preparation of WA. We would also like to thank the KUMC flow core facility for utilization of its resources established by a generous endowment from the Hall Foundation and by NIH Grant Number P20 RR016443 from the COBRE program of the National Center for Research Resources. We are thankful for research support provided by the Departments of Surgery at the

University of Kansas Medical Center and University of Michigan as well as the University of Michigan Comprehensive Cancer Center.

Role of Funding Sources: This work was made possible by support from the National Institutes of Health (NIH-COBRE P20 RR015563 P.I. B. Timmermann), the Institute for Advancing Medical Innovation (PI: MS Cohen), a University of Kansas Cancer Center Summer Student Training Program grant (PT Grogan), the Departments of Surgery at the University of Kansas Medical Center and University of Michigan (MS Cohen), and a University of Michigan Comprehensive Cancer Center CCSG Development award (PI: MS Cohen).

References

1. ACS. Cancer Facts and Figures 2013. American Cancer Society; Atlanta, GA: 2013. [cited 2013 November 20]
2. Gillingham FJ, Yamashita J. [The effect of radiotherapy for glioblastoma: a review of 516 cases (author's transl)]. No Shinkei Geka. 1975; 3(4):329–36. [PubMed: 174023]
3. Onoyama Y, et al. Radiation therapy in the treatment of glioblastoma. AJR Am J Roentgenol. 1976; 126(3):481–92. [PubMed: 178194]
4. Sheline GE. Radiation therapy of brain tumors. Cancer. 1977; 39(2 Suppl):873–81. [PubMed: 837351]
5. Stupp R, et al. Radiotherapy plus concomitant and adjuvant temozolomide for glioblastoma. N Engl J Med. 2005; 352(10):987–96. [PubMed: 15758009]
6. Stupp R, et al. Promising survival for patients with newly diagnosed glioblastoma multiforme treated with concomitant radiation plus temozolomide followed by adjuvant temozolomide. J Clin Oncol. 2002; 20(5):1375–82. [PubMed: 11870182]
7. DeAngelis LM. Chemotherapy for brain tumors--a new beginning. N Engl J Med. 2005; 352(10): 1036–8. [PubMed: 15758016]
8. Taphoorn MJ, et al. Health-related quality of life in patients with glioblastoma: a randomised controlled trial. Lancet Oncol. 2005; 6(12):937–44. [PubMed: 16321761]
9. Chamberlain MC, et al. Early necrosis following concurrent Temodar and radiotherapy in patients with glioblastoma. J Neurooncol. 2007; 82(1):81–3. [PubMed: 16944309]
10. Paz MF, et al. CpG island hypermethylation of the DNA repair enzyme methyltransferase predicts response to temozolomide in primary gliomas. Clin Cancer Res. 2004; 10(15):4933–8. [PubMed: 15297393]
11. Hegi ME, et al. MGMT gene silencing and benefit from temozolomide in glioblastoma. N Engl J Med. 2005; 352(10):997–1003. [PubMed: 15758010]
12. Hansen RJ, et al. Role of O6-methylguanine-DNA methyltransferase in protecting from alkylating agent-induced toxicity and mutations in mice. Carcinogenesis. 2007; 28(5):1111–6. [PubMed: 17116724]
13. Kitange GJ, et al. Induction of MGMT expression is associated with temozolomide resistance in glioblastoma xenografts. Neuro Oncol. 2009; 11(3):281–91. [PubMed: 18952979]
14. Quick A, et al. Current therapeutic paradigms in glioblastoma. Rev Recent Clin Trials. 2010; 5(1): 14–27. [PubMed: 20205684]
15. Chamberlain MC. Temozolomide: therapeutic limitations in the treatment of adult high-grade gliomas. Expert Rev Neurother. 2010; 10(10):1537–44. [PubMed: 20925470]
16. Zhang J, Stevens MF, Bradshaw TD. Temozolomide: mechanisms of action, repair and resistance. Curr Mol Pharmacol. 2012; 5(1):102–14. [PubMed: 22122467]
17. Wen PY, Kesari S. Malignant gliomas in adults. N Engl J Med. 2008; 359(5):492–507. [PubMed: 18669428]
18. Zhang H, et al. Antiproliferative withanolides from Datura wrightii. J Nat Prod. 2013; 76(3):445–9. [PubMed: 23252848]
19. Santagata S, et al. Using the heat-shock response to discover anticancer compounds that target protein homeostasis. ACS Chem Biol. 2012; 7(2):340–9. [PubMed: 22050377]
20. Hahm ER, et al. Withaferin A-Induced Apoptosis in Human Breast Cancer Cells Is Mediated by Reactive Oxygen Species. Plos One. 2011; 6(8)

21. Mayola E, et al. Withaferin A induces apoptosis in human melanoma cells through generation of reactive oxygen species and down-regulation of Bcl-2. Apoptosis. 2011; 16(10):1014–1027. [PubMed: 21710254]
22. Widodo N, et al. Selective killing of cancer cells by Ashwagandha leaf extract and its component Withanone involves ROS signaling. Plos One. 2010; 5(10):e13536. [PubMed: 20975835]
23. Malik F, et al. Reactive oxygen species generation and mitochondrial dysfunction in the apoptotic cell death of human myeloid leukemia HL-60 cells by a dietary compound withaferin A with concomitant protection by N-acetyl cysteine. Apoptosis. 2007; 12(11):2115–33. [PubMed: 17874299]
24. Oh JH, Kwon TK. Withaferin A inhibits tumor necrosis factor-alpha-induced expression of cell adhesion molecules by inactivation of Akt and NF-kappaB in human pulmonary epithelial cells. Int Immunopharmacol. 2009; 9(5):614–9. [PubMed: 19236958]
25. Koduru S, et al. Notch-1 inhibition by Withaferin-A: a therapeutic target against colon carcinogenesis. Mol Cancer Ther. 2010; 9(1):202–10. [PubMed: 20053782]
26. Yu Y, et al. Withaferin A targets heat shock protein 90 in pancreatic cancer cells. Biochem Pharmacol. 2010; 79(4):542–51. [PubMed: 19769945]
27. Stan SD, Zeng Y, Singh SV. Ayurvedic medicine constituent withaferin a causes G2 and M phase cell cycle arrest in human breast cancer cells. Nutr Cancer. 2008; 60(Suppl 1):51–60. [PubMed: 19003581]
28. Oh JH, et al. Induction of apoptosis by withaferin A in human leukemia U937 cells through down-regulation of Akt phosphorylation. Apoptosis. 2008; 13(12):1494–504. [PubMed: 19002588]
29. Mandal C, et al. Withaferin A induces apoptosis by activating p38 mitogen-activated protein kinase signaling cascade in leukemic cells of lymphoid and myeloid origin through mitochondrial death cascade. Apoptosis. 2008; 13(12):1450–64. [PubMed: 18987975]
30. Mohan R, et al. Withaferin A is a potent inhibitor of angiogenesis. Angiogenesis. 2004; 7(2):115–22. [PubMed: 15516832]
31. Singh D, et al. Withania somnifera inhibits NF-kappaB and AP-1 transcription factors in human peripheral blood and synovial fluid mononuclear cells. Phytother Res. 2007; 21(10):905–13. [PubMed: 17562568]
32. Samadi AK, et al. A novel RET inhibitor with potent efficacy against medullary thyroid cancer in vivo. Surgery. 2010; 148(6):1228–36. discussion 1236. [PubMed: 21134556]
33. Shah N, et al. Effect of the alcoholic extract of Ashwagandha leaves and its components on proliferation, migration, and differentiation of glioblastoma cells: combinational approach for enhanced differentiation. Cancer Sci. 2009; 100(9):1740–7. [PubMed: 19575749]
34. Grogan PT, et al. Cytotoxicity of withaferin A in glioblastomas involves induction of an oxidative stress-mediated heat shock response while altering Akt/mTOR and MAPK signaling pathways. Invest New Drugs. 2013; 31(3):545–557. [PubMed: 23129310]
35. Yang HJ, Shi GQ, Dou QP. The tumor proteasome is a primary target for the natural anticancer compound withaferin a isolated from “Indian Winter Cherry”. Molecular Pharmacology. 2007; 71(2):426–437. [PubMed: 17093135]
36. Stan SD, et al. Withaferin A causes FOXO3a- and Bim-dependent apoptosis and inhibits growth of human breast cancer cells in vivo. Cancer Research. 2008; 68(18):7661–7669. [PubMed: 18794155]
37. Devi PU, Kamath R, Rao BS. Radiosensitization of a mouse melanoma by withaferin A: in vivo studies. Indian J Exp Biol. 2000; 38(5):432–7. [PubMed: 11272405]
38. Samadi AK, et al. Natural withanolide withaferin A induces apoptosis in uveal melanoma cells by suppression of Akt and c-MET activation. Tumor Biology. 2012; 33(4):1179–1189. [PubMed: 22477711]
39. Fong MY, et al. Withaferin A synergizes the therapeutic effect of doxorubicin through ROS-mediated autophagy in ovarian cancer. PLoS One. 2012; 7(7):e42265. [PubMed: 22860102]
40. Munagala R, et al. Withaferin A induces p53-dependent apoptosis by repression of HPV oncogenes and upregulation of tumor suppressor proteins in human cervical cancer cells. Carcinogenesis. 2011; 32(11):1697–705. [PubMed: 21859835]

41. Nadkarni A, et al. ATM inhibitor KU-55933 increases the TMZ responsiveness of only inherently TMZ sensitive GBM cells. J Neurooncol. 2012; 110(3):349–57. [PubMed: 23054561]
42. Samadi AK, et al. Withaferin A, a cytotoxic steroid from Vassobia breviflora, induces apoptosis in human head and neck squamous cell carcinoma. J Nat Prod. 2010; 73(9):1476–81. [PubMed: 20726569]
43. Samadi AK, et al. A novel C-terminal HSP90 inhibitor KU135 induces apoptosis and cell cycle arrest in melanoma cells. Cancer Lett. 2011; 312(2):158–67. [PubMed: 21924824]
44. Ryu CH, et al. Valproic acid downregulates the expression of MGMT and sensitizes temozolomide-resistant glioma cells. J Biomed Biotechnol. 2012; 2012:987495. [PubMed: 22701311]
45. Puputti M, et al. Amplification of KIT, PDGFRA, VEGFR2, and EGFR in gliomas. Mol Cancer Res. 2006; 4(12):927–34. [PubMed: 17189383]
46. Wullich B, et al. Amplified met gene linked to double minutes in human glioblastoma. Eur J Cancer. 1993; 29A(14):1991–5. [PubMed: 8280494]
47. Berezowska S, Schlegel J. Targeting ErbB receptors in high-grade glioma. Curr Pharm Des. 2011; 17(23):2468–87. [PubMed: 21827413]
48. Potti A, et al. Determination of HER-2/neu overexpression and clinical predictors of survival in a cohort of 347 patients with primary malignant brain tumors. Cancer Invest. 2004; 22(4):537–44. [PubMed: 15565811]
49. Guessous F, et al. An orally bioavailable c-Met kinase inhibitor potently inhibits brain tumor malignancy and growth. Anticancer Agents Med Chem. 2010; 10(1):28–35. [PubMed: 20015006]
50. Zhang WB, et al. Activation of AMP-activated protein kinase by temozolomide contributes to apoptosis in glioblastoma cells via p53 activation and mTORC1 inhibition. J Biol Chem. 2010; 285(52):40461–71. [PubMed: 20880848]
51. Ansari N, Khodagholi F, Amini M. 2-Ethoxy-4,5-diphenyl-1,3-oxazine-6-one activates the Nrf2/HO-1 axis and protects against oxidative stress-induced neuronal death. Eur J Pharmacol. 2011; 658(2-3):84–90. [PubMed: 21371450]
52. Qiao S, et al. Thiostrepton is an inducer of oxidative and proteotoxic stress that impairs viability of human melanoma cells but not primary melanocytes. Biochemical Pharmacology. 2012; 83(9):12.
53. Khan S, Rammeloo AW, Heikkila JJ. Withaferin A induces proteasome inhibition, endoplasmic reticulum stress, the heat shock response and acquisition of thermotolerance. PLoS One. 2012; 7(11):e50547. [PubMed: 23226310]
54. D'Atri S, et al. Attenuation of O(6)-methylguanine-DNA methyltransferase activity and mRNA levels by cisplatin and temozolomide in jurkat cells. J Pharmacol Exp Ther. 2000; 294(2):664–71. [PubMed: 10900246]
55. Hirose Y, et al. Delayed repletion of O6-methylguanine-DNA methyltransferase resulting in failure to protect the human glioblastoma cell line SF767 from temozolomide-induced cytotoxicity. J Neurosurg. 2003; 98(3):591–8. [PubMed: 12650433]
56. Weller M, et al. Prolonged survival with valproic acid use in the EORTC/NCIC temozolomide trial for glioblastoma. Neurology. 2011; 77(12):1156–1164. [PubMed: 21880994]
57. Sztajnkrycer MD. Valproic acid toxicity: Overview and management. Journal of Toxicology-Clinical Toxicology. 2002; 40(6):789–801. [PubMed: 12475192]
58. Baer JC, et al. Depletion of O6-alkylguanine-DNA alkyltransferase correlates with potentiation of temozolomide and CCNU toxicity in human tumour cells. Br J Cancer. 1993; 67(6):1299–302. [PubMed: 8512814]
59. Kaina B, Margison GP, Christmann M. Targeting O(6)-methylguanine-DNA methyltransferase with specific inhibitors as a strategy in cancer therapy. Cell Mol Life Sci. 2010; 67(21):3663–81. [PubMed: 20717836]
60. Zheng M, et al. Interleukin-24 overcomes temozolomide resistance and enhances cell death by down-regulation of O6-methylguanine-DNA methyltransferase in human melanoma cells. Mol Cancer Ther. 2008; 7(12):3842–51. [PubMed: 19056673]
61. Citti L, et al. Targeting of O6-methylguanine-DNA methyltransferase (MGMT) activity by antimessenger oligonucleotide sensitizes CHO/Mex+ transfected cells to mitozolomide. Carcinogenesis. 1996; 17(1):25–9. [PubMed: 8565132]

62. Kreth S, et al. In human glioblastomas transcript elongation by alternative polyadenylation and miRNA targeting is a potent mechanism of MGMT silencing. Acta Neuropathol. 2013; 125(5): 671–81. [PubMed: 23340988]

63. Xie SM, et al. Silencing of MGMT with small interference RNA reversed resistance in human BCUN-resistant glioma cell lines. Chin Med J (Engl). 2011; 124(17):2605–10. [PubMed: 22040411]

64. Strik HM, et al. Temozolomide dosing regimens for glioma patients. Curr Neurol Neurosci Rep. 2012; 12(3):286–93. [PubMed: 22437507]

65. Rogakou EP, et al. Initiation of DNA fragmentation during apoptosis induces phosphorylation of H2AX histone at serine 139. J Biol Chem. 2000; 275(13):9390–5. [PubMed: 10734083]

66. Grover A, et al. Hsp90/Cdc37 chaperone/co-chaperone complex, a novel junction anticancer target elucidated by the mode of action of herbal drug Withaferin A. BMC Bioinformatics. 2011; 12(Suppl 1):S30. [PubMed: 21342561]

67. Fu J, et al. Autophagy induced by valproic acid is associated with oxidative stress in glioma cell lines. Neuro-Oncology. 2010; 12(4):328–340. [PubMed: 20308311]

68. Laurent A, et al. Controlling tumor growth by modulating endogenous production of reactive oxygen species. Cancer Research. 2005; 65(3):948–56. [PubMed: 15705895]

69. Cabello CM, Bair WB 3rd, Wondrak GT. Experimental therapeutics: targeting the redox Achilles heel of cancer. Curr Opin Investig Drugs. 2007; 8(12):1022–37.

70. Lee JJ, et al. PTEN status switches cell fate between premature senescence and apoptosis in glioma exposed to ionizing radiation. Cell Death Differ. 2011; 18(4):666–77. [PubMed: 21072054]

71. Koul D. PTEN signaling pathways in glioblastoma. Cancer Biology & Therapy. 2008; 7(9):1321–5. [PubMed: 18836294]

72. Lino MM, Merlo A. PI3Kinase signaling in glioblastoma. J Neurooncol. 2011; 103(3):417–27. [PubMed: 21063898]

73. Wu J, et al. Vitamin K3-2,3-epoxide induction of apoptosis with activation of ROS-dependent ERK and JNK protein phosphorylation in human glioma cells. Chem Biol Interact. 2011; 193(1): 3–11. [PubMed: 21453688]

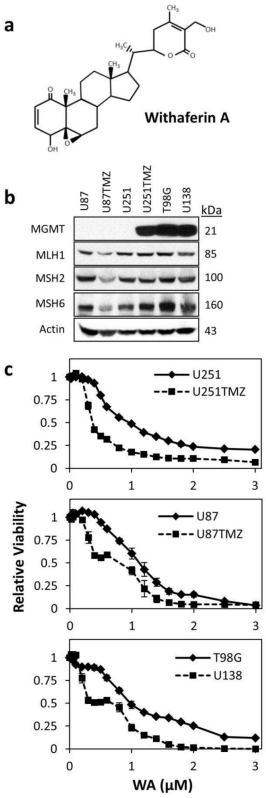

Fig. 1.

(a) 28-carbon steroidal lactone structure of withaferin A. (b) Characterization of TMZ-resistant cells U251TMZ, U87TMZ, T98G, and U138 compared to parental U251 and U87 cells. U251 and U87 cell lines demonstrated the absence of MGMT and the presence of mismatch repair proteins MLH1, MSH2, and MSH6. MGMT expression was observed in U251TMZ, T98G, and U138 cells but not U87TMZ. U87TMZ displayed lower levels of all three MMR proteins screened compared to parental U87 cells. (c) All cell lines were incubated with increasing concentrations of WA for 72h and then assessed by MTS assay. WA dose escalation reduced cell proliferation and viability with IC_{50} values of 0.766±0.045μM, 0.357±0.019μM, 1.050±0.062μM, 0.657±0.134μM, 1.027±0.105μM, and 0.610±0.279μM for U251, U251TMZ, U87, U87TMZ, T98G, and U138 cells, respectively.

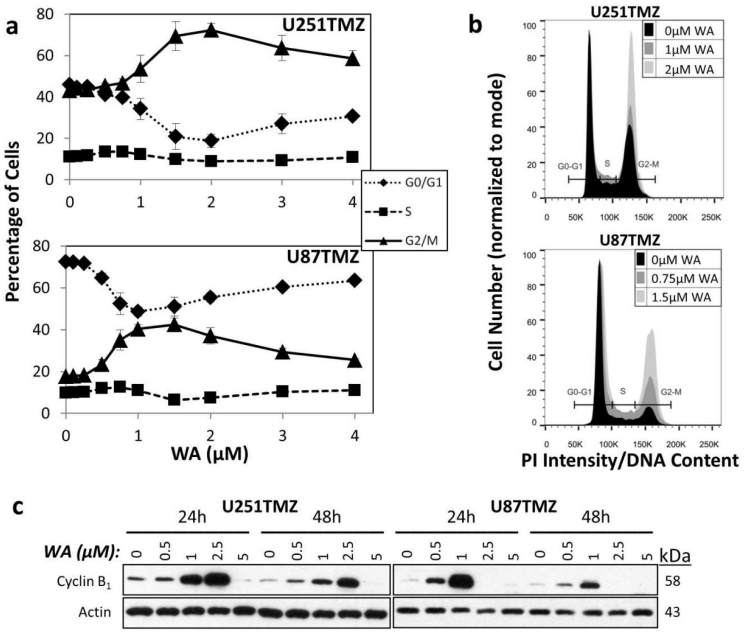

Fig. 2.

(a) Ability to induce cell cycle modulation was assessed by flow cytometry at 24h revealing that WA treatment results in dose-dependent G2/M cell cycle arrest. Maximum arrest was observed at 2μM and 1.5μM for U251TMZ and U87TMZ cells, respectively. (b) Histograms demonstrate cell cycle distribution for U251TMZ and U87TMZ cells at concentrations up to those yielding maximal arrest. (c) Arrest in G2/M phase was molecularly confirmed by immunoblotting for cyclin B_1 at 24-48h. Highest levels of cyclin B_1 were observed at 2.5μM and 1μM WA for U251TMZ and U87TMZ cells, respectively, confirming flow cytometry findings.

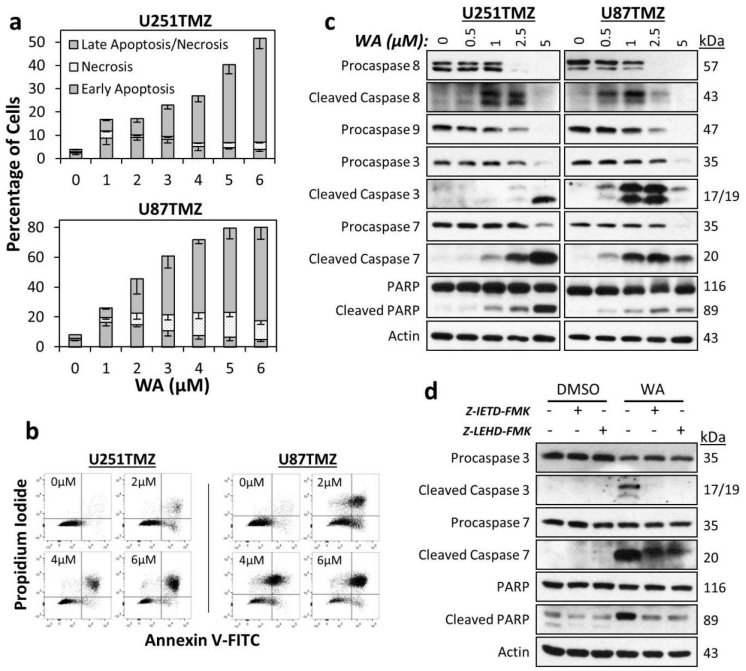

Fig. 3.

(a) WA treatment induced apoptotic cell death in U251TMZ and U87TMZ cells with increasing concentrations. 1-3μM WA induced early apoptotic processes with increasing levels of late apoptosis observed at all concentrations examined. Only U87TMZ demonstrated elevated necrosis with treatment. (b) Dot plots demonstrating propidium iodide and Annexin V-FITC staining show representative examples from both cell lines utilized. (c) An apoptotic mechanism was confirmed by Western blotting for total and cleaved initiator caspases 8 and 9, effector caspases 3 and 7, and downstream PARP. Uncleaved proteins were decreased with increasing WA concentration. U251TMZ and U87TMZ cells demonstrated optimal concentrations for caspase cleavage with highest levels of PARP cleavage observed in both lines at 5μM WA. (d) U251TMZ cells were pretreated with 50μM of either caspase 8 inhibitor ZIETD-FMK or caspase 9 inhibitor Z-LEHD-FMK for 1h followed by 2.5μM WA for 24h to determine if WA-driven apoptosis was intrinsically or extrinsically mediated. Inhibition of both caspase 8 and 9 reduced WA-induced cleavage of caspases 3 and 7 as well as PARP.

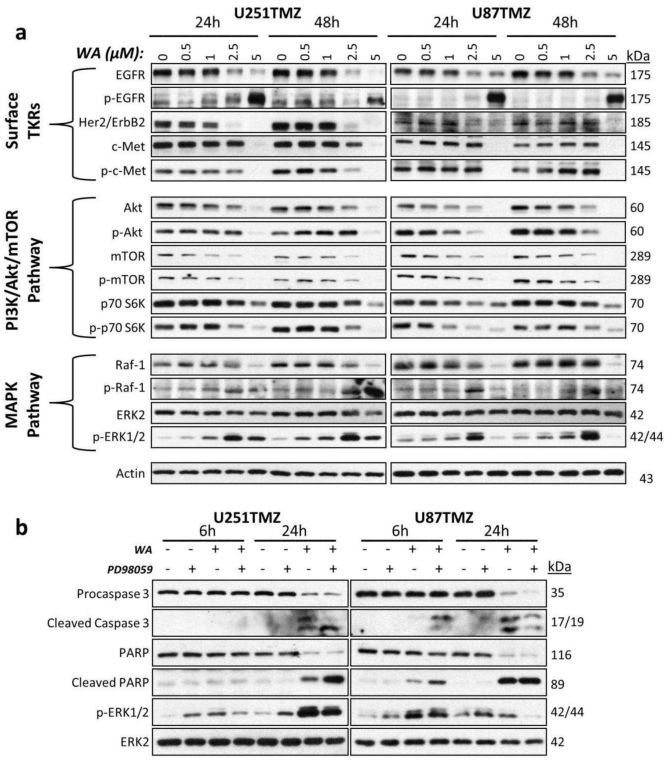

Fig. 4.

(a) Key proteins of the survival and proliferation PI3K/Akt/mTOR and MAPK pathways as well as common surface tyrosine kinase receptors were evaluated by immunoblotting for total levels and activation by phosphorylation following treatment with WA at 24-48h in U251TMZ and U87TMZ cells. Total levels of specific proteins in both pathways were decreased, but reduction of protein activation was only observed in the PI3K/Akt/MAPK pathway whereas phosphorylation of Raf-1 and ERK1/2 was increased. (b) To determine the nature of MAPK pathway activation, U251TMZ and U87TMZ cells were pretreated with 50μM of the MEK inhibitor PD98059 for 1h followed by 2.5μM WA for 6h or 24h. PD98059 increased ERK1/2 phosphorylation but reduced WA-induced phosphorylation of ERK1/2 in a time-dependent manner. WA alone induced caspase 3 and PARP cleavage in both cell lines in a time-dependent manner that was increased when combined with MEK inhibitor. This demonstrates that MAPK pathway activation with WA was acting in a pro-survival signal rather than contributing to apoptosis.

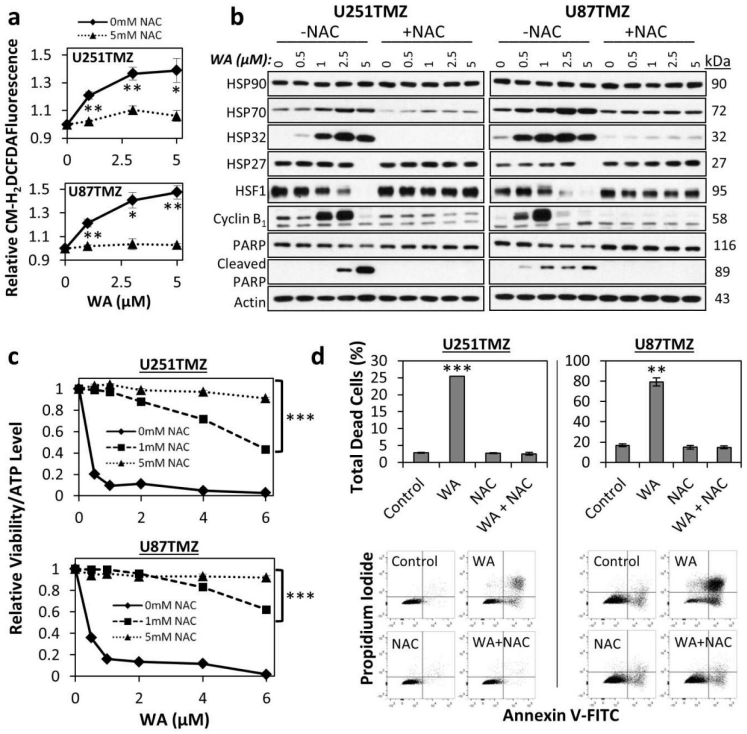

Fig. 5.

(a) The peroxide ROS indicator CM-H_2DCFDA was preloaded into U251TMZ and U87TMZ cells prior to WA exposure to determine alterations in oxidative potential. Elevations in signal that were observed with increasing concentrations of WA at 3h were reduced or completely absent with co-treatment of 5mM NAC. (b) Treatment with WA resulted in the induction of an NAC-repressible cellular stress heat shock response. Proteins associated with cellular stress and heat shock were evaluated by immunoblotting at 24h and revealed elevated levels of HSP32 and HSP70, known to be upregulated in response to oxidative stress, but decreased transcription factor HSF1 with increasing WA exposure that could be completely eliminated with 5mM NAC pretreatment. NAC also prevented induction of cyclin B_1 and cleavage of PARP. Functionally, NAC pretreatment reduced the anti-proliferative (c) and procytotoxic (d) effects of WA as assessed by the CellTiter-Glo assay at 72h and flow cytometry at 24h, respectively. *$p < 0.05$, **$p < 0.01$, ***$p < 0.001$

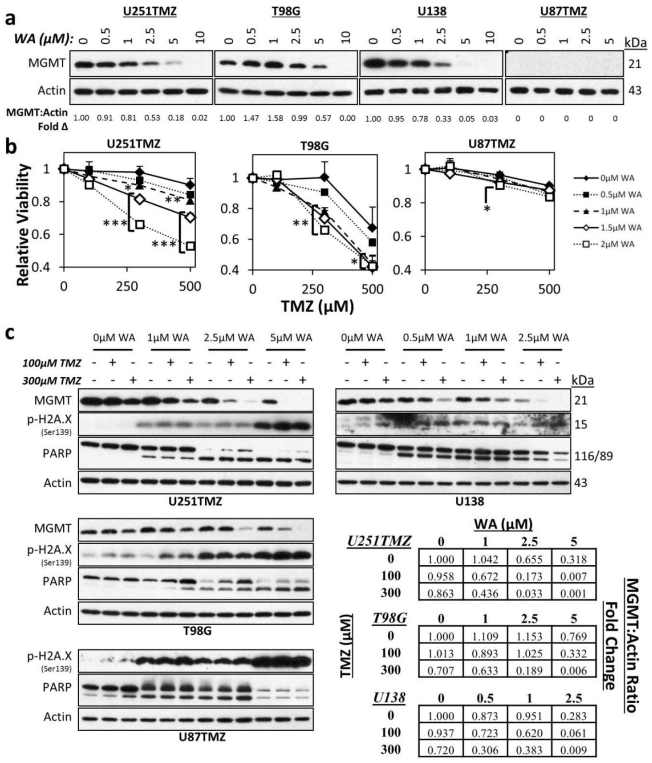

U251TMZ	0	1	2.5	5
0	1.000	1.042	0.655	0.318
100	0.958	0.672	0.173	0.007
300	0.863	0.436	0.033	0.001

T98G	0	1	2.5	5
0	1.000	1.109	1.153	0.769
100	1.013	0.893	1.025	0.332
300	0.707	0.633	0.189	0.006

U138	0	0.5	1	2.5
0	1.000	0.873	0.951	0.283
100	0.937	0.723	0.620	0.061
300	0.720	0.306	0.383	0.009

Fig. 6.

(a) WA treatment reduced protein levels of MGMT in TMZ-resistant U251TMZ, T98G, and U138 cell lines at 48h. MGMT was not observed in U87TMZ. (b) 24h pretreatment with WA resensitized MGMT-expressing U251TMZ and T98G cells to TMZ in a dose-dependent manner as assessed by a normalized MTS assay, but no resensitization was observed in MGMT-deficient U87TMZ cells. (c) TMZ-resistant cells were treated with WA for 24h followed by TMZ exposure for an additional 24h. Pretreatment with WA potentiated and/or synergized with TMZ to induce further depletion of MGMT in MGMT-expressing lines. Increasing WA concentrations yielded higher levels of p-H2A.X and cleaved PARP in all cell lines, but only T98G demonstrated WA-mediated increased levels with TMZ exposure. *$p < 0.05$, **$p < 0.01$, ***$p < 0.001$